Spatial control of spin-wave modes in $Ni_{80}Fe_{20}$ antidot lattices by embedded Co nanodisks

G. Duerr,[1] M. Madami,[2] S. Neusser,[1] S. Tacchi,[2] G. Gubbiotti,[2,3] G. Carlotti,[2] and D. Grundler[1,a)]

[1]*Lehrstuhl für Physik funktionaler Schichtsysteme, Technische Universität München, Physik Department, James-Franck-Str. 1, D-85747 Garching b. München, Germany*
[2]*CNISM, Unità di Perugia and Dipartimento di Fisica, Via A. Pascoli, I-06123 Perugia, Italy*
[3]*Istituto Officina dei Materiali del CNR (CNR-IOM), Unità di Perugia, c/o Dipartimento di Fisica, Via A. Pascoli, I-06123 Perugia, Italy*

(Received 7 June 2011; accepted 26 October 2011; published online 15 November 2011)

Combined all-electrical spin-wave and micro-focused Brillouin light scattering spectroscopies have been used to study spin-wave eigenmodes in bicomponent lattices formed by periodic Co nanodisks introduced in nanotroughs etched into a thin $Ni_{80}Fe_{20}$ film. We find two characteristic spin-wave modes extending through the lattice perpendicular to the applied field. Their spatial positions depend crucially on the Co nanodisks as they reverse locally the polarity of the internal field. Embedded nanodisks are found to offer control of spin waves at nearly the same eigenfrequency in periodically patterned magnetic devices and magnonic crystals. © *2011 American Institute of Physics*. [doi:10.1063/1.3662841]

Starting from the pioneering work by Vasseur *et al.*,[1] magnonic crystals (MCs) have gained considerable interest because of the large possibility of tuning and optimizing the magnonic band structure.[2] Periodically patterned nanodevices have already shown interesting spin wave transmission properties.[3–6] A 1D MC consisting of alternating Co and $Ni_{80}Fe_{20}$ nanostripes exhibited allowed minibands and forbidden frequencies gaps, i.e., MC behavior.[4] Such 1D bicomponent periodic lattices thus offered an unprecedented control of spin wave properties in one spatial direction. It is now interesting to explore experimentally bicomponent lattices periodically patterned in two dimensions,[1,7] leading to an additional degree of freedom in manipulating spin wave properties. In this letter we report on the spin dynamics of a two-dimensional array of Co nanodisks embedded in a thin film of $Ni_{80}Fe_{20}$ (Py). We investigate them using all-electrical spin-wave spectroscopy (AESWS),[5] micro-focused Brillouin light scattering (μBLS),[8] and micromagnetic simulations.[9] When applying an in-plane magnetic field H along a high symmetry direction we find two different spin wave modes extending through the lattice instead of the one recently found in pure Py antidot lattices.[5,10–12] Depending on the eigenfrequency two modes exist in parallel stripes going either through Co nanodisks or the Py effective stripes existing between them. Such binary component magnetic lattices thus offer additional degrees of freedom to control magnonic devices if compared with the previously published antidot lattices (ADLs) incorporating etched holes.[5,10–12]

Samples were based on 300 μm by 120 μm large Py mesas [see Fig. 1(b)] of 26 nm thickness deposited on a semi-insulating GaAs substrate using electron gun evaporation. Subsequently a square lattice of circular nanotroughs was etched into the Py using a resist mask prepared by electron beam lithography and Ar ion milling. The troughs were 7 nm deep and refilled with 15 nm thick Co in the same vacuum chamber without breaking the vacuum. After lift-off processing a bicomponent nanodisk/antidot lattice was obtained [Figs. 1(a) and 1(c)]. We prepared different bicomponent periodic lattices and report here on sample 1 where the lattice constant amounted to 1 μm. The disks were 435 nm$\pm$ 10 nm in diameter. As a reference sample we prepared a nanotrough-based antidot lattice without Co (sample 2) from the same Py [Fig. 1(d)]. Note that earlier investigations addressed etched-through ADLs.[5,10–12] Silicon dioxide was sputtered onto the samples to provide an electrical isolation for two open-ended metallic coplanar waveguides (CPWs) integrated by lift-off processing [Fig. 1(b)]. The resulting six conducting lines [inset of Fig. 1(b)] were 4 μm wide and 2.4 μm apart resulting in separation of 19.2 μm between the two signal lines marked S1 and S2. CPWs were connected to a vector network analyzer to perform AESWS as presented in Ref. 5. Following Ref. 13 we estimated the maximum excitation strength to occur at a wave vector $k = 3.6 \times 10^3$ rad/cm. An in-plane magnetic field H was applied to study the field dependence of magnetic modes. We evaluated the scattering parameter S_{21} measured between two neighboring CPWs after subtraction of a reference dataset.[5] μBLS was used to spatially map the profile of the spin precession amplitude.[14] A monochromatic light ($\lambda = 532$ nm) was focused down to a 235 nm spot diameter by using a 100$\times$ dark field Zeiss objective (NA = 0.75).[8] The precession amplitudes of the modes were resonantly enhanced by applying the relevant microwave frequency to the CPW. The same setup, through an additional illumination system and a CCD camera, allowed us to visualize the sample surface. Micromagnetic simulations were performed using the MicroMagus simulation package.[9] For Py a saturation magnetization of $M_{sat,Py} = 806$ kA/m was used as determined experimentally. For Co, $M_{sat,Co} = 1000$ kA/m was chosen which provided best agreement with experimental data. An exchange constant of $A_{Py} = 13 \times 10^{-12}$ J/m was used for Py and $A_{Co} = 30 \times 10^{-12}$ J/m for Co. We considered a damping coefficient of $\alpha = 0.01$. No anisotropy was considered in the simulations. Spin dynamics was induced by a field pulse of 4 mT amplitude applied perpendicular to the in-plane field

a)Electronic mail: grundler@ph.tum.de.

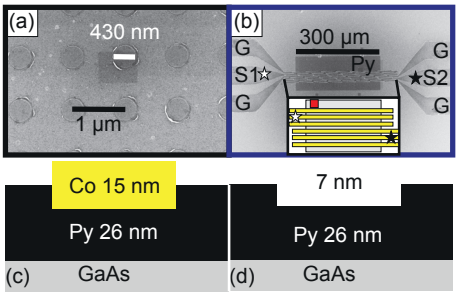

FIG. 1. (Color online) (a) Scanning electron microscopy image of sample 1 consisting of Co nanodisks (dark) in a 26 nm thick Py film (bright) on GaAs. The dark square is an artefact. (b) CPWs on top of the magnetic mesa (dark). The label G (S) denotes a ground (signal) line. Schematic cross sections of (c) Co/Py sample 1 and (d) Py sample 2. Seven nanometer deep troughs were etched into both samples. For sample 1, 15 nm thick Co nanodisks were deposited *in situ*.

pointing 45° out-of-plane in order to reproduce the in- and out-of-plane components of the CPWs field. Simulations were performed at a wavevector $k = 0$, i.e., we used uniform excitation. The simulated unit cell was composed of 256 by 256 pixels resulting in a pixel edge length of 3.9 nm.

In Fig. 2 we show AESWS and μBLS data acquired on samples 1 and 2 as grey-scale plots and symbols (left) and compare them to micromagnetic simulations (right column). Dark color indicates large microwave absorption. The external field H is applied along the edge of the squared unit cell parallel to the CPWs. The sample has been saturated before each single measurement using $\mu_0 H = 100$ mT. In the bicomponent Co/Py sample 1 we observe up to five modes depending on H. The resonances shift to higher frequency with increasing H [Fig. 2(a)]. A similar shift is observed for the reference Py sample 2 without Co [Fig. 2(b)] where we resolve only two modes. Compared with the micromagnetic simulations depicted in Figs. 2(c) and 2(d) we find that experimental and simulated data agree reasonably well. The field dependencies are remodeled, and the simulations consistently predict more modes for Co nanodisks embedded in a Py film (sample 1) if compared to the pure Py sample with

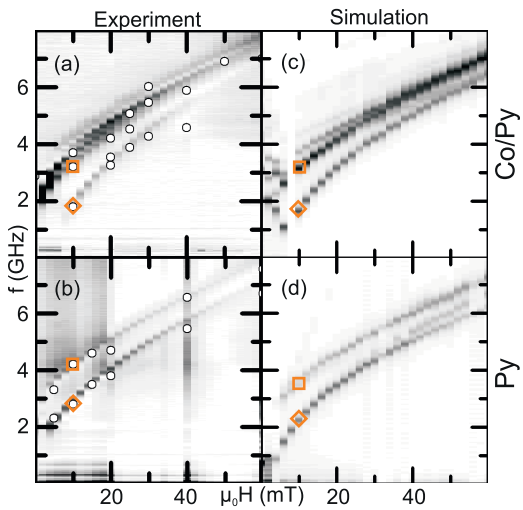

FIG. 2. (Color online) Measured (left) and simulated (right) spin wave resonances of the Co/Py sample 1 [(a) and (c)] and Py sample 2 [(b) and (d)]. AESWS (BLS) data are presented as grey-scale plots (circles). The in-plane field was applied along the edge of the squared unit cell. Open squares and diamonds mark the modes addressed in Fig. 3.

periodic nanotroughs (sample 2). Remaining discrepancies in absolute frequencies are attributed to imperfections of the samples such as rough edges of the shallow-etched troughs and the residual crystalline anisotropy of the polycrystalline Co grown on the etched Py. These features have not been considered in the simulations. Interestingly, for both samples the relevant frequency regime is similar. Eigenfrequencies are always between about 2 and 8 GHz in Fig. 2.

In the following, we use μBLS intensity maps and micromagnetic simulations from Fig. 3 to explain the modes marked with squares and diamonds in Fig. 2. These were the two modes with the highest BLS intensity. We measured 2D maps of precession amplitudes by scanning the laser spot over an array of 2 μm by 2 μm with steps of 100 nm. The position of the scanning area is indicated by a red square in the inset of Fig. 1(b). The measured intensities have been normalized to compensate for the attenuation of the spin waves as a function of the distance from the CPW. To excite spin wave modes a microwave generator, tuned to the selected frequency, has been connected to one of the CPWs. When excited at 1.8 GHz, in Fig. 3(a), we find large spin precession amplitudes (i.e., large BLS signals) in parallel stripes (bright color) oriented perpendicular to both the CPW and the applied field $\mu_0 H = 10$ mT. The center-to-center separation of such stripes amounts to 1 μm, i.e., the lattice constant. Note that, when we excite at 3.2 GHz and scan over the same segment of the Co/Py sample we find extended stripes as well in Fig. 3(b). However, they are shifted by 500 nm along the direction of H if compared to Fig. 3(a). Stripes of large and vanishing spin precession amplitudes have changed the positions from (a) to (b). Two complementary stripe configurations in (a) and (b) are substantiated by the corresponding micromagnetic simulations shown in (c) and (d).[15] Notably the lower frequency excitation resides throughout and under the Co nanodisks. The positions of the Co nanodisks in Figs. 3(a) and 3(b) are indicated by dashed circles as they are seen by the μBLS optical visualization system. For sample 2 in Figs. 3(e) and 3(f) we show BLS data at 2.8 and 4.2 GHz, respectively, with measured nanotrough positions. The precession profiles look similar to Figs. 3(a) and 3(b). However, they are found at interchanged positions if compared to sample 1. Now, the low frequency mode resides between rows of

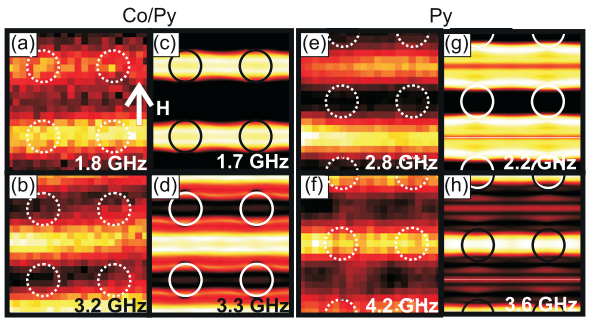

FIG. 3. (Color online) Measured spin precession profiles ($2 \times 2\,\mu m^2$) obtained by μBLS (first and third column) and simulated ones (second and fourth column). $\mu_0 H = 10$ mT is applied along the white arrow. The outer edge of the CPWs ground line is at the left edge of each graph. Co/Py sample 1 (Py sample 2) is shown in graphs (a) through (d) [(e) through (h)]. Relevant frequencies are given. Dotted circles in (a), (b), (e), and (f) are nanotrough positions extracted from microscopy.

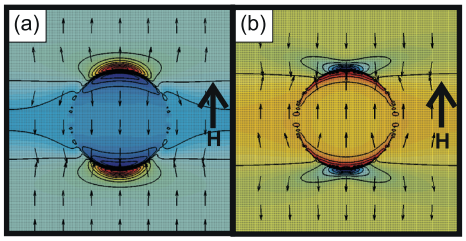

FIG. 4. (Color online) Simulated H_{dem} for (a) Co/Py sample 1 and (b) Py sample 2. Arrows show the direction of H_{dem}. Color and contour lines encode the intensity of H_{dem} projected on H (large arrow). The nearly horizontal contour lines extending from left to right represent $H_{dem} = 0$. Further lines encode variations in steps of 10 mT.

etched nanotroughs whereas the high frequency mode exhibits the large spin precession amplitude along etched regions. This is substantiated by the micromagnetic simulations in Figs. 3(g) and 3(h). Two coexisting stripe-like extended modes which are shifted by half the lattice constant have not yet been reported for pure Py ADLs.[5,10–12]

The striking difference between sample 1 and 2 is now elucidated further in terms of the demagnetization field H_{dem}, thereby following works on etched ADLs.[5,10–12] In Figs. 4(a) and 4(b) we depict H_{dem} of sample 1 and 2, respectively, as extracted from micromagnetic simulations. We find that in the bicomponent Co/Py sample 1 the central row containing the Co nanodisks exhibits a field H_{dem} which is opposite to H. This is in contrast to etched-through ADLs where H_{dem} is aligned with H in the corresponding row. The embedded nanodisks lead to stripes of reduced internal field explaining the stripe-like low frequency excitation of Fig. 3(a). In the horizontal stripes above and below the Co nanodisk row, H_{dem} is aligned with H. Such stripes of the periodic lattice thus experience a large internal field, i.e., large eigenfrequency as observed in Fig. 3(b). The scenario is contrary for the pure Py sample 2 where the local orientations of H_{dem} in Fig. 4(b) are, in particular, opposite to the ones found in Fig. 4(a). As a consequence the spin wave mode extending in continuous Py regions has a lower frequency. The introduction of Co nanodisks thus allows one to actively control H_{dem} at the nanoscale and change its polarity to tailor spin-wave excitations.

In conclusion we observed that a periodic array of shallow-etched holes in Py provoke two stripe-like spin-wave excitations which extend in a direction perpendicular to the applied field. Depending on the frequency they exist between the rows of etched nanotroughs or extend through them. Filling the nanotroughs with Co shifts their positions in the periodic lattice. Already in the non-optimized lattices explored here the eigenfrequencies experienced by the shifted modes stay almost the same at a given field. Periodic lattices with segments of filled and empty nanotroughs thus allow one to spatially shift magnonic excitations within the given lattice and potentially optimize spin-wave transmission coefficients across interfaces between neighboring magnonic devices consisting of antidot lattices.

The research leading to these results has received funding from the European Community's Seventh Framework Programme (FP7/2007-2013) under Grant Agreement No. 228673 MAGNONICS. Financial support by the German Excellence Cluster Nanosystems Initiative Munich (NIM) and CNISM under the μBLS Innesco project is gratefully acknowledged.

[1]J. O. Vasseur, L. Dobrzynski, B. Djafari-Rouhani, and H. Puszkarski, Phys. Rev. B **54**, 1043 (1996).
[2]A. V. Chumak, T. Neumann, A. A. Serga, B. Hillebrands, and M. P. Kostylev, J. Phys. D: Appl. Phys. **42**, 205005 (2009).
[3]G. Gubbiotti, S. Tacchi, G. Carlotti, N. Singh, S. Goolaup, A. O. Adeyeye, and M. Kostylev, Appl. Phys. Lett. **90**, 092503 (2007).
[4]Z. K. Wang, V. L. Zhang, H. S. Lim, S. C. Ng, M. H. Kuok, S. Jain, and A. O. Adeyeye, ACS Nano **4**, 643 (2010).
[5]S. Neusser, G. Duerr, H. G. Bauer, S. Tacchi, M. Madami, G. Woltersdorf, G. Gubbiotti, C. H. Back, and D. Grundler, Phys. Rev. Lett. **105**, 067208 (2010).
[6]S. Tacchi, F. Montoncello, M. Madami, G. Gubbiotti, G. Carlotti, L. Giovannini, R. Zivieri, F. Nizzoli, S. Jain, A. O. Adeyeye, and N. Singh, Phys. Rev. Lett. **107**, 127204 (2011).
[7]F. S. Ma, H. S. Lim, Z. K. Wang, S. N. Piramanayagam, S. C. Ng, and M. H. Kuok, Appl. Phys. Lett. **98**, 153107 (2011).
[8]G. Gubbiotti, G. Carlotti, M. Madami, S. Tacchi, P. Vavassori, and G. Socino, J. Appl. Phys. **105**, 07D521 (2009).
[9]D. V. Berkov and N. L. Gorn, Micromagus, software for micromagnetic simulations.
[10]S. Neusser, B. Botters, and D. Grundler, Phys. Rev. B **78**, 054406 (2008).
[11]S. Neusser, B. Botters, M. Becherer, D. Schmitt-Landsiedel, and D. Grundler, Appl. Phys. Lett. **93**, 122501 (2008).
[12]C.-L. Hu, R. Magaraggia, H.-Y. Yuan, C. S. Chang, M. Kostylev, D. Tripathy, A. O. Adeyeye, and R. L. Stamps, Appl. Phys. Lett. **98**, 262508 (2011).
[13]K. J. Kennewell, M. Kostylev, and R. L. Stamps, J. Appl. Phys. **101**, 09D107 (2007).
[14]M. Madami, S. Tacchi, G. Gubbiotti, G. Carlotti, F. Montoncello, G. Capuzzo, and F. Nizzoli, J. Phys.: Conf. Ser. **200**, 042008 (2010).
[15]Spatial fast Fourier transformation maps for sample 1 (sample 2) have been extracted from the simulation layer containing, both, Co and Py (in the continuous Py layer). No significant differences have been found for other layers.